Supporting Information

Three-dimensional ZnO@MnO_2 core@shell nanostructures for electrochemical energy storage

Xing Sun,[a] Qiang Li,[ab] Yinong Lü[c] and Yuanbing Mao*[a]

[a] Department of Chemistry, University of Texas - Pan American, Edinburg, TX 78539 USA

[b] Department of Mechanical Engineering, University of Texas - Pan American, Edinburg, TX 78539 USA

[c] College of Materials Science and Engineering, Nanjing University of Technology, Nanjing 210009, China

*To whom correspondence should be addressed: Phone: +1 956 665 2417; Fax: +1 956 665 5006; E-mail: maoy@utpa.edu

Experimental Section

Synthesis: To highlight the advantages of our smartly designed 3D nanoforest architecture over the most recently engineered 3D nanowire arrays reported in the literature, two different 3D nanostructures, i.e. ZnO@MnO_2 core@shell nanowire arrays and ZnO@MnO_2 nanoforests, were synthesized by the same procedure and their electrochemical performance was compared. The only difference on the synthetic procedure is that one extra step was taken to grow ZnO branches onto ZnO nanowire arrays to form the ZnO nanoforests. The fabrication procedures are illustrated in Scheme 1. Specifically, ZnO nanowire arrays and nanoforests were synthesized according to a modified procedure based on a previous report.[1]

In the first step, the ZnO nanowire backbones were grown based on a previously reported hydrothermal process with modified synthesis conditions: ammonia added into the precursor solution.[2] First, a seed solution of ZnO nanoparticles was obtained through adding 25 mL of 0.03 M sodium hydroxide (NaOH) ethanol solution into 37.5 mL of 0.01 M zinc acetate [$Zn(O_2CCH_3)_2 \cdot 2H_2O$] ethanol solution drop by drop, and then the mixture was actively stirred at 60 ^oC for 2 h. The seed solution was drop casted onto a titanium substrate. ZnO nanowire arrays were grown from these ZnO nanoparticle seeds through immersing in an aqueous precursor solution containing 0.025 M zinc nitrate hydrate [$Zn(NO_3)_2 \cdot 6H_2O$], 0.025 M hexamethylenetetramine ($C_6H_{12}N_4$, HMTA), 0.1 M polyethylenimine (PEI), and 0.15 M ammonia ($NH_3 \cdot H_2O$) at 60~90 ^oC for 7~15 h. The length of ZnO nanowire arrays can be controlled by altering reaction time, temperature and concentration of precursor solution. Then these grown ZnO nanowire arrays were thoroughly rinsed with deionized water, and dried in air. After annealed at 350 ^oC in air for 10 min to remove residual organics (mostly PEI), ZnO nanowire arrays on Ti substrate were obtained. Robust adherence between ZnO nanowire arrays and titanium substrate was guaranteed by an annealing step at 350 ^oC for 10 min.

ZnO nanoforests were synthesized as follow: ZnO nanoparticle seed solution was first added onto the surface of the as-prepared ZnO nanowire arrays by a similar drop casting process, and subsequently a similar hydrothermal reaction was conducted as described above except without adding ammonia or PEI to grow ZnO nanorods as branches onto the ZnO nanowire array trunks.

To fabricate the 3D ZnO@MnO_2 core@shell nanowire arrays and ZnO@MnO_2 nanoforests, ZnO@C nanowire arrays and nanoforests were obtained through immersing the respective as-obtained ZnO nanowire arrays and nanoforests into glucose aqueous solution (0.03 M) for 1 h and then annealed in argon atmosphere at 500 ^oC for 3 h. This annealing step carbonizes the glucose molecules absorbed onto the surfaces of ZnO nanowire arrays and nanoforests. Subsequently, electroactive MnO_2 nanoparticle coatings were decorated onto these ZnO nanowire arrays and nanoforests through immersing them into 0.03 M $KMnO_4$ aqueous solution for 1 h at room temperature. A thin layer of MnO_2 nanoparticles was grown on the 3D ZnO nanostructures through the redox reaction between the carbon coating on the ZnO nanoarchitectures with the $KMnO_4$ solution: $4MnO_4^- + 3C + H_2O = 4MnO_2 + CO_3^{2-} + 2HCO^{3-}$. At last, the MnO_2 nanoparticles coated ZnO nanowire arrays and nanoforests were rinsed with deionized water and dried at 80 ^oC overnight in vacuum.[3, 4]

Materials characterization*:* The morphology and crystal structure of the ZnO@MnO_2 nanowire arrays and nanoforests were characterized through scanning electron microscopy (Carl Zeiss Sigma VP Field-Emission SEM at 2~5 kV), transmission electron microscopy (JEOL JEM-2010 UHR TEM) and high-resolution TEM (HRTEM), coupled with selected area electron diffraction (SAED) and energy dispersive X-ray spectroscopy (EDS). The surface chemical composition and oxidation state of the samples were determined by X-ray photoelectron spectroscopy (XPS) measurement (Kratos AXIS 165 X-ray photoelectron spectrometer). Raman spectroscopy was conducted on a Bruker SENTERRA RAMAN microscope with a 785 nm laser as the excitation source.

Electrochemical measurement*:* Cyclic voltammetry (CV) measurements were conducted on a Gamry Reference 600 electrochemical workstation, using a three-electrode mode in 1 M Na_2SO_4 aqueous solution with a voltage ranging from -0.2 V to 0.6 V at different scan rates (2 mV/s to 100 mV/s). A piece of 0.6 cm^2 electrode of the as-synthesized 3D ZnO@MnO_2 nanowire arrays or nanoforests grown on titanium foil substrate was used as the working electrode. The reference electrode and counter electrode were Ag/AgCl and a platinum wire, respectively. With the same setup, charge/discharge (CD) measurements of the 3D ZnO@MnO_2 nanowire arrays or nanoforests as working electrodes were conducted at various current densities of 0.02 to 0.2 mA/cm^2. Electrochemical impedance spectroscopy (EIS) measurements were performed by applying an AC amplitude of 5 mV in a frequency range from 100 kHz to 0.001 Hz.

Scheme 1. Schematic illustration of the fabrication process for the designed 3D ZnO@MnO_2 core@shell nanowire array electrode and the nanoforest counterpart. The latter possesses further boosted electrochemical performance than the former.

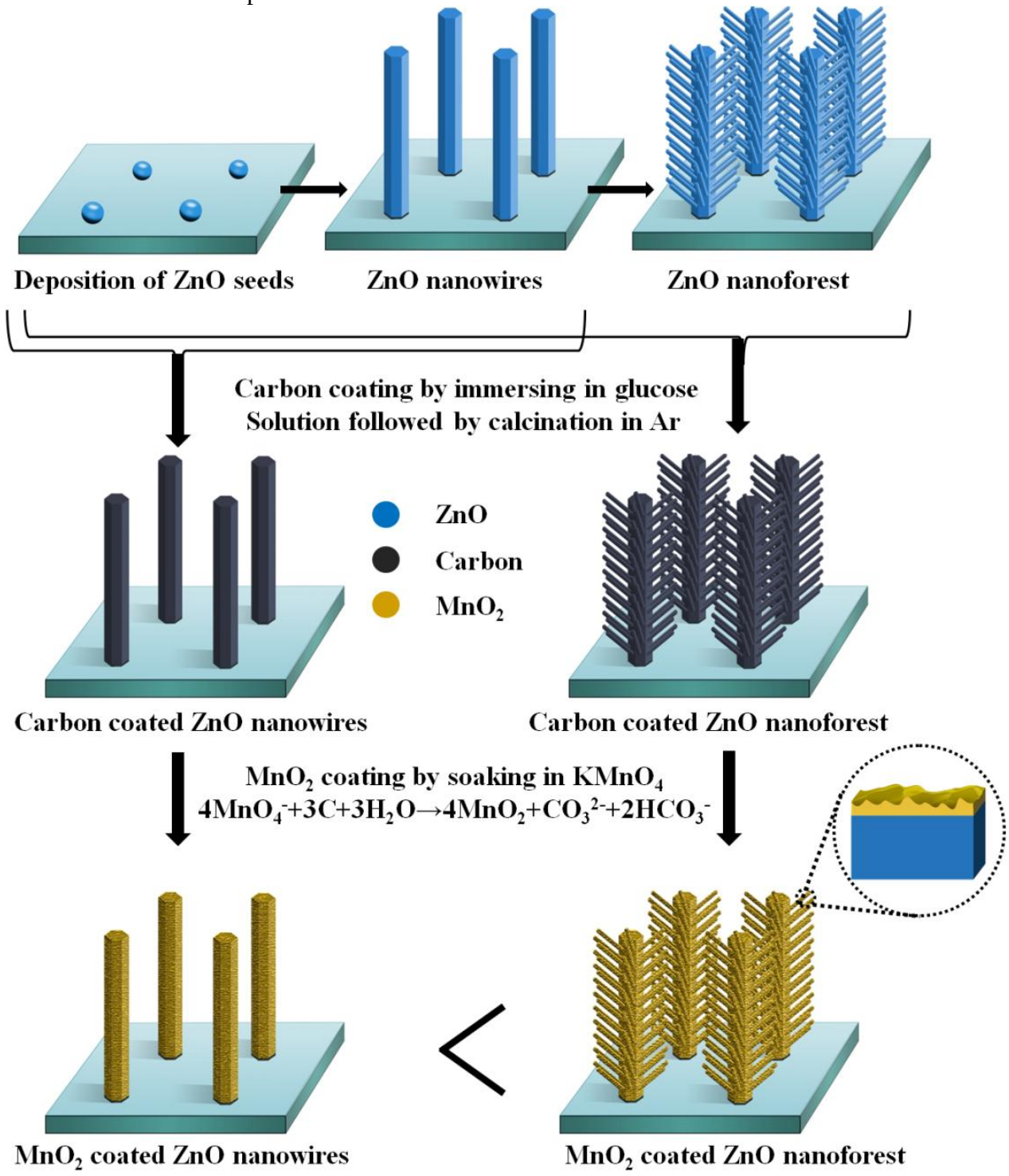

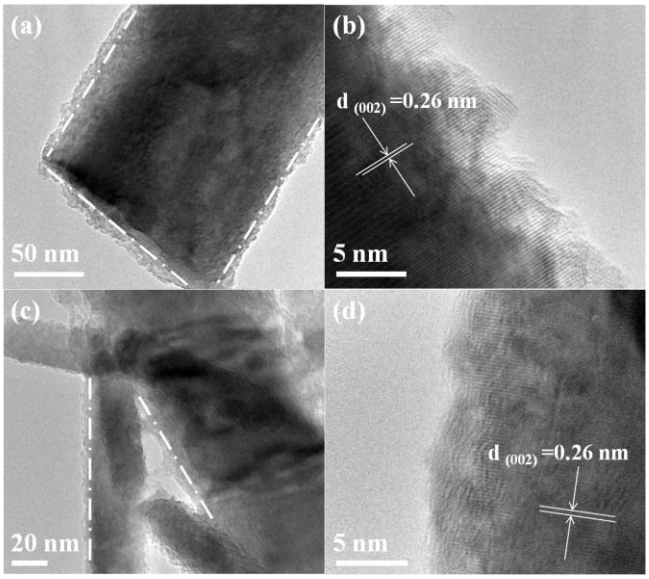

Fig. S1 Representative TEM images of the synthesized 3D ZnO@MnO_2 core@shell (a and b) nanowire arrays and (c and d) nanoforests: (a) TEM image taken from the end of an individual nanowire; (b) HRTEM image focusing on the edge of an individual nanowire shown in (a); (c) TEM image taken from one part of an individual branched nanowire; (d) HRTEM image focusing on the edge of an individual branched nanowire shown in (c).

Fig. S1a and S1b exhibit TEM and HRTEM images of an individual ZnO@MnO_2 core@shell nanowire, respectively. These images clearly demonstrate that a well-dispersed MnO_2 nanoparticle layer with a thickness of ~3 nm was coated on the entire surface of the single crystalline ZnO nanowire backbone. Fig. S1c and S1d show a portion of an individual 3D ZnO@MnO_2 core@shell nanotree. The electroactive MnO_2 shell coating is also about 3 nm thick and uniformly covers the surface of the branched ZnO nanotree backbone since the electroactive MnO_2 coating was done by the same fabricating procedure for both the 3D ZnO@MnO_2 core@shell nanowire arrays and forest of nanotrees.

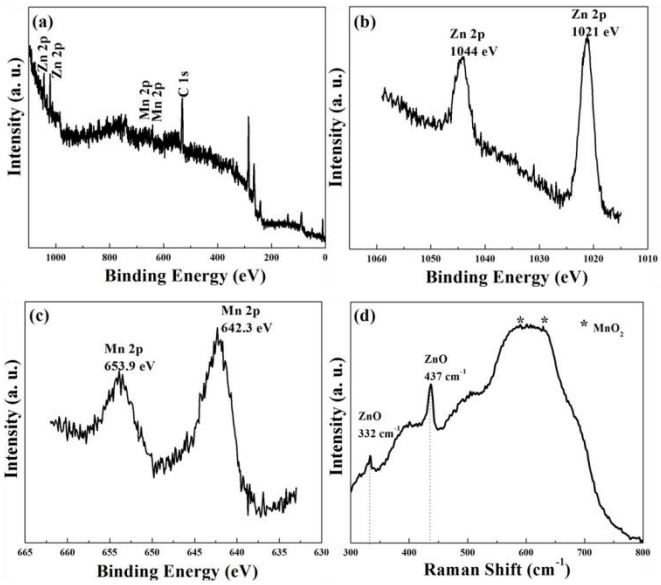

Fig. S2 (a) Overview XPS spectrum of the as-synthesized 3D ZnO@MnO_2 core@shell nanoforests; detailed XPS data taken from the synthesized 3D ZnO@MnO_2 core@shell nanoforests: (b) the spectrum of Zn 2*p*, (c) the spectrum of Mn 2*p*; (d) Raman spectrum of the as-synthesized 3D ZnO@MnO_2 core@shell nanoforests.

The overview XPS spectrum (Fig. S2a) demonstrates the presence of zinc (Zn 2*p*), manganese (Mn 2*p*), oxygen (O 1*s*) as well as carbon (C 1*s*). The element zinc, manganese and oxygen signals are originated from the ZnO core and MnO_2 shell, which is in agreement with the EDS results (Fig. S3). The carbon peak may come from air exposure during sample preparation or incomplete redox reaction between carbon and $KMnO_4$ during the synthesis. The Raman peaks centered at 332 and 437 cm^{-1} are indexed to crystalline ZnO. Raman bands at 629 and 578 cm^{-1} are respectively related to the symmetric stretching vibration (Mn-O) of the MnO_6 groups and the (Mn-O) stretching vibration in the basal plane of MnO_6 sheet.[5, 6]

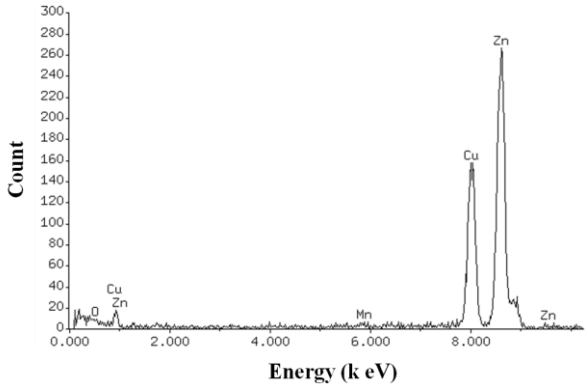

Fig. S3 Energy-dispersive X-ray spectroscopy (EDS) data taken from the as-synthesized 3D ZnO@MnO_2 core@shell nanoforests shown in Figure S1c.

The EDS peaks of zinc, manganese, copper and oxygen are displayed in this spectrum. The copper peaks come from the TEM sample grid, and no peaks of other elements are observed. It further confirms that the 3D ZnO@MnO_2 core@shell nanoforest is composed of Zn, Mn, and O, consistent with the XPS results shown in Figures S2.

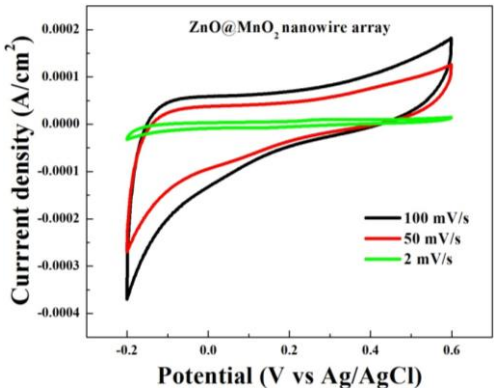

Fig. S4 Cyclic Voltammetry (CV) curves of the as-synthesized 3D ZnO@MnO_2 nanowire arrays as the working electrode at different scan rates.

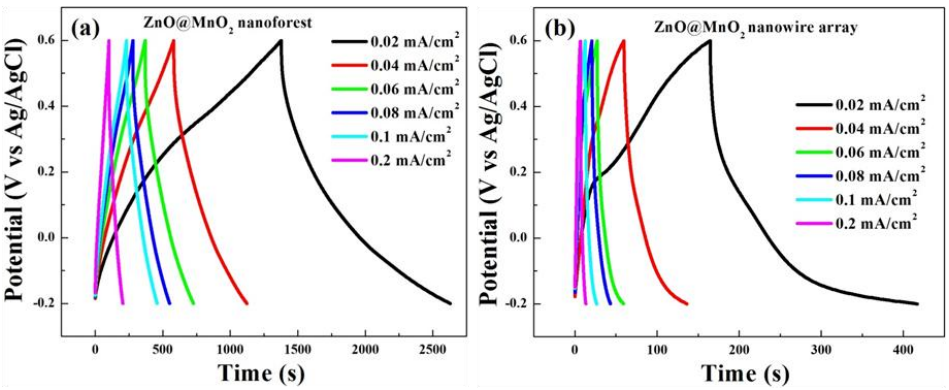

Fig. S5 (a) Charge/discharge (CD) curves of the as-synthesized 3D ZnO@MnO_2 nanoforests as the working electrode at different current densities (from 0.02 mA/cm^2 to 0.2 mA/cm^2). (b) CD curves of the as-synthesized ZnO@MnO_2 nanowire arrays as the working electrode at current densities from 0.02 mA/cm^2 to 0.2 mA/cm^2.

The CD curves of the as-synthesized 3D ZnO@MnO_2 nanoforests at current densities of 0.02, 0.04, 0.06, 0.08, 0.1 and 0.2 mA/cm^2 show good symmetry, indicating good electrochemical characteristics and superior reversible reactions.

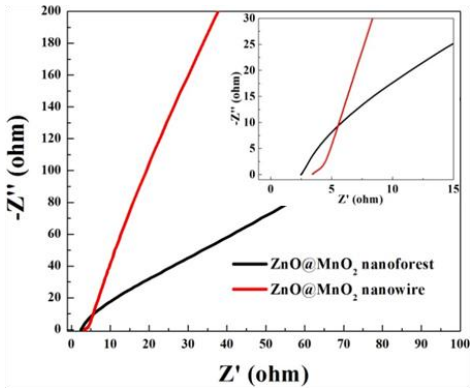

Fig. S6 EIS results of the synthesized 3D ZnO@MnO_2 core@shell nanoforest and nanowire array electrodes.

The Nyquist plots corresponding to the electrochemical impedance spectra taken from the electrodes of the 3D ZnO@MnO_2 core@shell nanoforests and corresponding nanowire arrays are shown in Figure 5. It shows that the 3D ZnO@MnO_2 core@shell nanoforest electrodes (2.45 Ω) have smaller internal resistance than the corresponding nanowire array electrodes (3.45 Ω), based on the intercepts with the Z´ axis in the high frequency range (inset of Figure 5). This may be contributed from the interconnected growth of ZnO branches, and it is consistent with the higher capacitance and better capacitance retention of the former as discussed in the preceding sections. On the other hand, the 3D ZnO@MnO_2 core@shell nanoforest electrodes have a bigger Warburg resistance compared with the nanowire array counterparts, based on the slope of the EIS curves in the low frequency range. The possible reason for this difference may be the overgrowth of dense ZnO branches onto the ZnO nanotrees, especially on the bottom of the ZnO trunks. It slows down the diffusion of redox species in the electrolyte compared with the straight nanowire arrays in the 3D ZnO@MnO_2 core@shell nanowire array electrodes. Optimization of the synthetic procedure for the 3D ZnO nanoforest backbone will be able to overcome this issue in the future.

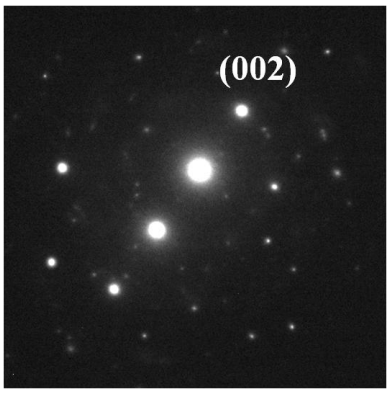

Fig. S7 SAED patterns of the as-synthesized 3D ZnO@MnO_2 core@shell (a) nanowire arrays and (b) nanoforests.

The SAED pattern can be indexed as hexagonal wurtzite structure of ZnO (JCPDS No. 80-75, *P*63*mc*, $a = b = 0.325$ nm, $c = 0.521$ nm). There is no MnO_2-related diffraction pattern or spot observed in this SAED pattern, which indicates that the MnO_2 coating is amorphous.

Table S1: Discharging capacitance retention of the as-synthesized 3D ZnO@MnO_2 core@shell nanoforests and corresponding nanowire arrays at different current densities in the voltage range of -0.2 to 0.6 V (vs Ag/AgCl).

Electrode types	Current density [mA/cm^2]	Discharge time [s]	Capacitance [mF/cm^2]	Discharging capacitance retention [%]
ZnO@MnO_2 nanoforests	0.02	1251.970	31.299	100
	0.04	564.263	28.213	90.140
	0.06	368.280	27.621	88.248
	0.08	280.985	28.098	89.773
	0.10	226.985	28.373	90.651
	0.20	108.765	27.191	86.875
ZnO@MnO_2 nanowire arrays	0.02	252.172	6.304	100
	0.04	76.7017	3.835	60.833
	0.06	32.185	2.414	38.289
	0.08	22.5917	2.259	35.835
	0.10	13.8717	1.734	27.504
	0.20	6.68167	1.670	26.497

Areal capacitance was calculated according to the equation (1):

$$C_{area} = \frac{i*t}{A*Vi} \quad (1)$$

where I is the discharge current, t is the discharge time, A is the effective area of an electrode, and V_i is the voltage interval of the charge-discharge measurements. The capacitance retention was calculated from the ratio of each specific capacitance of different current densities to that of lowest current density (0.02 mA/cm^2).

Reference

[1] S. H. Ko, D. Lee, H. W. Kang, K. H. Nam, J. Y. Yeo, S, J. Hong, C. P. Grigoropoulos and H. J. Sung, *Nano Lett*., 2011, **11**, 666.
[2] L. Y. Chen, Y. T. Yin, C. H. Chen and J. W. Chiou, *J. Phys. Chem. C*, 2011, **115**, 20913.
[3] Z. Fan, J. Yan, T. Wei, L. Zhi, G. Ning, T. Li, and F. Wei, *Adv. Funct. Mater*., 2011, **21**, 2366.
[4] J. Liu, J. Jiang, C. Cheng, H. Li, J. Zhang, H. Gong and H. J. Fan, *Adv. Mater*., 2011, **23**, 2076.
[5] J. Liu, J. Jiang, M. Bosman and H. J. Fan, *J. Mater. Chem*., 2012, **22**, 2419.
[6] C. Julien, M. Massot, R. Baddour-Hadjean, S. Franger, S. Bach and J. P. Pereira-Ramos, *Solid State Ionics*, 2003, **159**, 345.